Cerebral Cortex, July 2018;28: 2636–2646

doi: 10.1093/cercor/bhy093
Advance Access Publication Date: 21 April 2018
Original Article

ORIGINAL ARTICLE

Frontal Transcranial Direct Current Stimulation Induces Dopamine Release in the Ventral Striatum in Human

Clara Fonteneau[1,2,3], Jérome Redoute[4], Frédéric Haesebaert[1,2,3], Didier Le Bars[4,5,6], Nicolas Costes[4], Marie-Françoise Suaud-Chagny[1,2] and Jérome Brunelin[1,2,3]

[1]INSERM U1028, CNRS UMR5292, Lyon Neuroscience Research Center, Psychiatric Disorders: from Resistance to Response Team, F-69000 Lyon, France, [2]University Lyon 1, Villeurbanne, F-69000 Lyon, France, [3]Centre Hospitalier Le Vinatier, Lyon, F-69000 Lyon, France, [4]Centre d'Etude et de Recherche Multimodal et Pluridisciplinaire en Imagerie du Vivant (CERMEP-Imagerie du vivant), Lyon, F-69000 Lyon, Auvergne-Rhône-Alpes, France, [5]ICBMS, Université de Lyon, F-69000 Lyon, France and [6]Hospices Civils de Lyon, F-69000 Lyon, France

Address correspondence to Marie-Françoise Suaud-Chagny, Centre Hospitalier Le Vinatier, Equipe de Recherche PSYR2, Pôle Est – Bâtiment 416 – 1er étage, BP 300 39 – 95 boulevard Pinel, 69678 Bron Cedex, France. Email: Marie-Francoise.SUAUD-CHAGNY@ch-le-vinatier.fr

Marie-Françoise Suaud-Chagny and Jérome Brunelin contributed equally to this work.

Abstract

A single transcranial direct current stimulation (tDCS) session applied over the dorsolateral prefrontal cortex (DLFPC) can be associated with procognitive effects. Furthermore, repeated DLPFC tDCS sessions are under investigation as a new therapeutic tool for a range of neuropsychiatric conditions. A possible mechanism explaining such beneficial effects is a modulation of meso-cortico-limbic dopamine transmission. We explored the spatial and temporal neurobiological effects of bifrontal tDCS on subcortical dopamine transmission during and immediately after the stimulation. In a double blind sham-controlled study, 32 healthy subjects randomly received a single session of either active (20 min, 2 mA; $n = 14$) or sham ($n = 18$) tDCS during a dynamic positron emission tomography scan using [^{11}C]raclopride binding. During the stimulation period, no significant effect of tDCS was observed. After the stimulation period, compared with sham tDCS, active tDCS induced a significant decrease in [^{11}C]raclopride binding potential ratio in the striatum, suggesting an increase in extracellular dopamine in a part of the striatum involved in the reward–motivation network. The present study provides the first evidence that bifrontal tDCS induces neurotransmitter release in polysynaptic connected subcortical areas. Therefore, levels of dopamine activity and reactivity should be a new element to consider for a general hypothesis of brain modulation by bifrontal tDCS.

Key words: dopamine, dorsolateral prefrontal cortex, positron emission tomography, striatum, transcranial direct current stimulation

Introduction

Dopamine is involved in various cognitive processes such as reward-related processes (Bromberg-Martin et al. 2010; Haber and Knutson 2010), emotion regulation (Lindquist et al. 2012), and executive functions (Wise 2004; Monchi et al. 2006; Cools 2011), via the meso-cortico-limbic pathway. This major dopaminergic pathway links the ventral tegmental area of the midbrain, the limbic system (including the ventral striatum), and the prefrontal cortex (Haber and Knutson 2010). Moreover, dopamine abnormalities in this pathway have been shown in multiple conditions such as major depressive disorder (Price and Drevets 2012), substance-related and addictive disorder (Nutt et al. 2015), schizophrenia (Brunelin et al. 2013; Maia and Frank 2017), and in Parkinson's disease (Hanganu et al. 2015).

Interestingly, cognitive processes, and symptomatology of diseases involving dopamine have been shown sensitive to noninvasive brain stimulations techniques (NIBS) applied over the dorsolateral prefrontal cortex (DLPFC). Among current NIBS, transcranial direct current stimulation (tDCS) consists in applying a weak direct current between 2 electrodes, a cathode, and an anode, placed above the subject's scalp. Applied over the primary motor cortex, anodal tDCS induces excitatory effects, whereas cathodal stimulation results in inhibitory effects on motor cortex excitability. When the stimulation is applied continually during several minutes, the induced excitability changes last for up to an hour (Nitsche et al. 2005). From animal studies, it has been hypothesized that tDCS-mediated effects are related to a shift in neuronal resting membrane potential either toward depolarization and increased spontaneous neuronal firing at the anodal level and toward hyperpolarization and decreased firing at the cathode level (Bindman et al. 1964).

As such, tDCS is a technique emerging as having procognitive effects in healthy humans (Levasseur-Moreau et al. 2013) and a prospective therapy to decrease symptoms and improve cognition in patients with neurologic and psychiatric disorders (Kuo et al. 2014; Lefaucheur et al. 2017). Specifically, bifrontal tDCS, with the anode applied over the left DLPFC coupled with the cathode placed over the right DLPFC may induce beneficial emotional and attentional processing in healthy subjects (Mondino et al. 2015), as well as clinical improvements in several psychiatric conditions involving dopamine transmission abnormalities, such as major depressive disorder (Brunoni et al. 2016; Sampaio-Junior et al. 2018), substance-related and addictive disorder (Jansen et al. 2013), schizophrenia with predominant negative symptoms (Palm et al. 2016), and the cognitive alterations in Parkinson's disease (Leite et al. 2014). However, contradictory studies exist putting forward the importance of the study design, the individual variability, and the brain-state dependency in the results obtained in both cognitive (Horvath et al. 2015; Wörsching et al. 2017) and clinical studies (Brunoni et al. 2017; Loo et al. 2018). These discrepancies reinforce the need to better understand the spatial and temporal neurobiological effects of bifrontal tDCS. In the last decade, fMRI studies (Keeser et al. 2011; Pena-Gomez et al. 2012) and computational model analysis (Bai et al. 2014) highlighted subcortical effects of bifrontal tDCS reaching subcortical areas, such as dopaminergic areas. Offline studies also suggest that cortical stimulation by other NIBS approaches, such as a single session of high frequency transcranial magnetic stimulation (TMS) applied over the left DLPFC may evoke a dopamine release in the striatum (Strafella et al. 2001; Brunelin et al. 2011). However, the effect of a bifrontal tDCS on dopamine transmission is unknown.

The aim of this study was to test, in healthy subjects in a randomized placebo-controlled double blind study, the effects of a single session of bifrontal tDCS with the anode over the left DLPFC and the cathode over the right DLPFC on the subcortical dopaminergic transmission. These effects were explored online by positron emission tomography (PET) using dopaminergic D2 subtype receptor availability via [^{11}C]raclopride binding. We hypothesized that bifrontal tDCS can modulate subcortical dopaminergic transmission during and after the stimulation.

Methods and Materials

Subjects

Thirty-six healthy adults were included. Exclusion criteria were smoking, history of neurological and/or psychiatric illness, medical treatments (except for oral contraceptive), contraindications to MRI or tDCS, and pregnancy. Volunteers were asked not to have caffeine on the day of scanning. Procedures were reviewed, approved by the standing ethics committee (CPP SUD EST 6, AU1148; ANSM, A01405-42) and registered on ClinicalTrials.gov (NCT02402101). All subjects gave written informed consent after a detailed description of the study by the recruiting psychiatrist. Subjects were compensated 100 euros. Four subjects were excluded due to technical problems (see CONSORT Flow Diagram). Thirty-two subjects (mean age = 25.25 ± 3.55 years, $n = 16$ females) completed the study.

Experimental Design

This study is randomized, double blind and with 2-arm parallel groups, active ($n = 14$) versus sham ($n = 18$) bifrontal tDCS (Fig. 1A). The experiment visit at the CERMEP imaging center consisted in an anatomical MRI and a PET scan during which subjects received a single tDCS session. At baseline, subjects completed personality questionnaires: Life Orientation Test-Revised (LOT-R; Trottier et al. 2008), Motivation (Guay et al. 2003), Big Five Inventory (Plaisant et al. 2010). During the experiment visit, subjects completed before and after the PET scan a State-Trait Anxiety Inventory (STAI-YA; Spielberger et al. 1970) and a structured adverse effect of tDCS questionnaire (Brunoni et al. 2011). Blinding integrity was assessed by having subjects guess the nature of the received stimulation (active or sham). Results are provided in Table 1.

Transcranial Direct Current Stimulation

tDCS was applied using a standard equipment (NeuroConn DC Stimulator Plus, GmbH). The anode was placed with the center of the electrode over F3 (left DLPFC) and the cathode was located over F4 (right DLPFC), according to international 10/20 EEG electrodes placement system (Fig. 1B). Electrode size was 7*5, 35 cm^2. tDCS (either active of sham) was delivered at rest in a single session during a dynamic PET scan. The stimulation started 40 min after the injection of the tracer, lasted 20 min, with 30 s fade in/fade out periods, and was set at 2 mA in active mode. For sham stimulation, the built-in sham mode mimicked the somatosensory artifact of active tDCS (30 s fade in/fade out, 40 s of active tDCS delivered at the beginning of stimulation).

Anatomical MRI

All subjects underwent an anatomical MRI examination performed on a 1.5-T Magnetom scanner (Siemens), including a 3-D anatomic T1-weighted sequence covering the whole brain volume, with 1-mm^3 cubic voxels and 176 1-mm thick slices (TR = 1970 ms, TE = 3.93 ms). This scan was done before PET

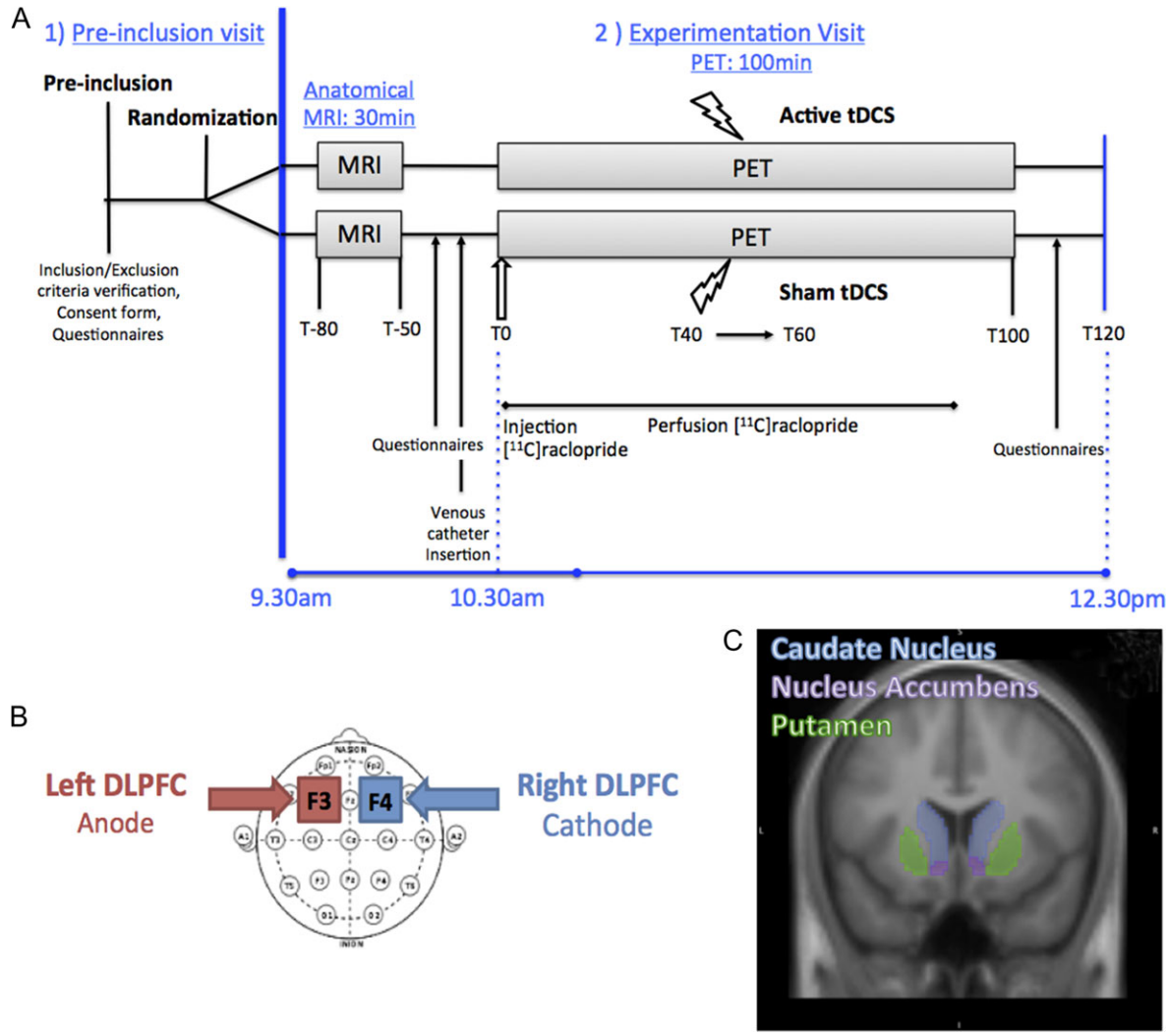

Figure 1. (A) Study design. (B) Transcranial direct current stimulation bifrontal montage. (C) Hammersmith maximum probability brain atlas used as a striatal mask including the caudate nucleus, putamen, and nucleus accumbens. Abbreviations: DLPFC, Dorsolateral prefrontal cortex; tDCS, transcranial direct current stimulation.

scan to control subject anatomy, electrode position and was further used for spatial normalization and to define the regions of interest (ROI).

Positron Emission Tomography

PET scan session always started around 10.30 a.m. During the 100-min PET acquisition, subjects were lying at rest in the machine.

Radiochemistry

Raclopride is a benzamide, a selective D2 receptor antagonist labeled with carbon-11, commonly used in PET studies (Hall et al. 1988). After synthesis at the CERMEP (1 synthesis per subject), [^{11}C]raclopride was purified, formulated, and sterilized. The specific radioactivity obtained was around 3.7–18.5 GBq/μmol (100–500 mCi/μmol) at the time of injection.

Data Acquisition

PET scans were conducted on a Biograph mCT PET-CT tomograph (Siemens). Subjects were positioned in the scanner such that acquired planes would be parallel to the orbital-meatal line. Head movement was minimized with an airbag. A camera allowed visual control of the head's position during acquisition. Measures for tissue and head support attenuation were performed with a 1 min low-dose CT scan acquired before emission data acquisition. A bolus of [^{11}C]raclopride (18 MBq + 2.6 MBq/kg) for 30 s followed by a constant infusion of 57% of the initial dose (i.e., 10 MBq + 1.5 MBq/kg) over 100 min, was injected through an intravenous catheter (see doses in Table 1). This bolus-plus-continuous-infusion method is currently used when measuring dopamine release in challenging conditions (Adler et al. 2000; Brunelin et al. 2011). A dynamic emission scan was acquired in list mode during the 100-min after injection. A total of 20 successive frames (5 min each) were reconstructed by using 3D-ordinary Poisson-ordered subset expectation maximization iterative algorithm incorporating point spread function and time of flight (with a Gaussian filter of 3 mm) after correction for scatter and attenuation. Reconstructed volumes consisted of 109 contiguous slices (2.03-mm thickness) of 128 × 128 voxels (2.12 × 2.12 mm^2). Actual resolutions for reconstructed images were approximately 2.6 mm in full width at half maximum in the axial direction and 3.1 mm in full width at half maximum in the transaxial direction measured for a source located 1 cm from the field of view (Jakoby et al. 2011).

Table 1 Characteristics of subjects among the 2 groups (active and sham tDCS; mean (±SD))

Variable	Active tDCS (N = 14)	Sham tDCS (N = 18)	P-value
Demographic			
Age [years]	24.86 (±4.05)	25.56 (±3.18)	0.3886
Sex [Male:Female]	6:8	10:8	0.7216
Years of education [years]	3.92 (±1.86)	4.78 (±1.83)	0.2077
Handedness [Right:Left]	12:2	13:5	0.6278
PET scan			
Injected dose [MBq/kg]	320.86 (±35.02)	320.33 (±59.10)	0.7812
Movement translation [mm]	−0.20 (±1.38)	−0.13 (±1.79)	0.2792
Movement rotation [degrees]	0.004 (±0.011)	0.004 (±0.012)	0.8879
Psychological assessment			
Motivation score	123.79 (±21.00)	124.06 (±15.90)	0.9684
LOT-R score	17.86 (±3.35)	15.72 (±14.86)	0.1525
BFI N score	17.64 (±5.57)	20.72 (±7.06)	0.1781
Baseline STAI-A score	25.5 (±4.07)	26.61 (±5.25)	0.5794
Post-tDCS STAI-A score	24.71 (±4.34)	26.56 (±3.49)	0.1173
STAI-A score difference	0.79 (±3.47)	0.05 (±3.90)	0.5803
Blinding [Active:Sham:None]	6:6:2	5:13:0	0.1203

Abbreviations: BFI N, Big Five Inventory Neuroticism; LOT-R, Life Orientation Test-Revised; STAI-YA, State-Trait Anxiety Inventory (form Y-A, anxiety state); tDCS, transcranial Direct Current Stimulation. Welch 2 sample *t*-test or Wilcoxon rank sum test with continuity correction and the chi-square tests were conducted to assess group differences for continuous and discrete variables, respectively.

Data Preprocessing and Binding Parametric Imaging

All preprocessing were carried out by a single individual blind to group status (active or sham). For each subject, preprocessing of MRI and PET data was done using an in-house script combining functions of Statistical Parametric Mapping 12 (SPM12, Wellcome Trust Centre of Neuroimaging), the MINC Tool Kit (Mc Connell brain Imaging centre, McGill University), and the Turku PET analysis software (Turku PET Centre). PET dynamic was corrected for between-frame motion with a 3-D rigid body model using SPM12. This realigned dynamic PET scan was used hereon out. T1 was coregistered to the mean PET image for each subject and then spatially normalized into standard MNI space (Montreal Neurological Institute/International Consortium for Brain Mapping stereotactic space) with the "segment" function of SPM12. This step provided a classification of the T1 MRI into 6 tissue classes and generation of MNI to subject space deformation fields. The atlas was then back normalized into the subject space, and combined with the gray matter image. The assessment of free and nonspecific [^{11}C]raclopride ligand kinetics was based on the time–activity curve of a reference region (i.e., the cerebellum, without vermis) devoid of specific dopamine D2-like receptors (Pinborg et al. 2007). Thus, extracellular dopamine concentration was assessed using simple pseudo-equilibrium 5 min ratios of ROI (striatum) to cerebellum activities (BP_R), computed with the "imgratio" function of the Turku PET library. BP_R images were spatially normalized into the standard MNI space and smoothed using an isotropic 8-mm full width half maximum Gaussian kernel. ROIs were selected from the Hammersmith maximum probability brain atlas (Hammers et al. 2003; Gousias et al. 2008). The a priori ROI used in this study is the striatum. This ROI was used for subsequent regional BP_R and used as mask in the SPM analysis. The anatomical subparts of the striatum (i.e., caudate nucleus, putamen, and nucleus accumbens; Fig. 1*C*) were used only after the analysis to name the significant clusters accordingly.

Statistical Analyses

A voxel-based SPM analysis was performed, using a flexible factorial design based on repeated measures ANOVA, to assess the effect of active tDCS compared with sham tDCS on BP_R for each time period: baseline period (30–40 min), stimulation period (45–60 min, effects during stimulation), Post1 period (65–80 min, acute after-effects), and Post2 period (80–95 min, subsequent after-effects). This analysis was restricted to voxels belonging to the striatum mask (a priori ROI). In SPM12, used in the present study, contrasts (post hoc) can be performed only when the omnibus ANOVA created with the model is significant (Friston et al. 1991). Post hoc Student *t*-score (SPM-{*t*}) maps were computed to elucidate the increase or decrease of [^{11}C]raclopride uptake during (Stimulation time period) or after (Post1 and Post2 time periods) tDCS, by comparing active and sham groups. The following contrasts were computed: $[(\text{Stimulation}-\text{Baseline})_{\text{sham}}$ vs. $(\text{Stimulation}-\text{Baseline})_{\text{active}}]$, $[(\text{Post1}-\text{Baseline})_{\text{sham}}$ vs. $(\text{Post1}-\text{Baseline})_{\text{active}}]$, $[(\text{Post2}-\text{Baseline})_{\text{sham}}$ vs. $(\text{Post2}-\text{Baseline})_{\text{active}}]$, $[((\text{Post1}+\text{Post2})-\text{Baseline})_{\text{sham}}$ vs. $((\text{Post1}+\text{Post2})-\text{Baseline})_{\text{active}}]$, $[((\text{Stimulation}+\text{Post1}+\text{Post2})-\text{Baseline})_{\text{sham}}$ vs. $((\text{Stimulation}+\text{Post1}+\text{Post2})-\text{Baseline})_{\text{active}}]$, $[(\text{Post1}-\text{Stimulation})_{\text{sham}}$ vs. $(\text{Post1}-\text{Stimulation})_{\text{active}}]$, $[(\text{Post2}-\text{Stimulation})_{\text{sham}}$ vs. $(\text{Post2}-\text{Stimulation})_{\text{active}}]$, $[(\text{Post1}-\text{Post2})_{\text{sham}}$ vs. $(\text{Post1}-\text{Post2})_{\text{active}}]$, $[((\text{Post1}+\text{Post2})-\text{Stimulation})_{\text{sham}}$ vs. $((\text{Post1}+\text{Post2})-\text{Stimulation})_{\text{active}}]$. SPM maps were thresholded at $P_{\text{uncorr}} < 0.001$ at the voxel level, with a minimum of 10 contiguous voxels (80 mm^3), which is the expected number of voxels per cluster in the 3D gaussian space. Then, only clusters with $P_{\text{FWE}} < 0.05$ (SPM family wised error correction for multiple comparisons) at the cluster level were considered significant. Reported coordinates (Table 2) conform to the MNI space, for each cluster. Time–activity curves were extracted for each cluster and the BP_R value computed in each time period and for each group. BP_R were also expressed as the relative difference between groups at each time periods (Table 3). A secondary analysis was performed in order to investigate the potential impact of dopamine baseline levels (BP_R) on the relative changes (Delta (%)) observed in the significant cluster, with a correlation analysis (Pearson's *r* correlation coefficient). $P < 0.05$ was considered significant. Demographic and clinical characteristics were examined using descriptive statistics. Normality was assessed by the Shapiro–Wilk test. Statistical analyses were done between groups using the Welch 2 sample *t*-test (Injected dose/kg, Years of

Table 2 Parametric analysis: group comparison

Contrast/region	MNI coordinates (mm)				Cluster	
	x	y	z	z-Score	P_{FWE}	Volume (mm^3)
(Stimulation + Post1 + Post2)–Baseline						
right caudate nucleus	10	14	4	4.06	0.037	272
(Post1 + Post2)–Baseline						
Right caudate nucleus	10	14	4	4.28	0.023	352
(Post1 + Post2)–Stimulation						
Right caudate nucleus	6	16	−4	3.49	0.092	144
Left putamen	−28	2	−2	3.65	0.081	160
Post1–Stimulation						
Right caudate and accumbens nuclei	6	12	−4	4.17	0.092	144
Left putamen	−30	2	−6	3.53	0.064	192
Post2–Baseline						
Right caudate nucleus	10	14	4	4.40	0.022	360
Left putamen	−22	10	−12	3.47	0.105	128
Post2–Stimulation						
Right caudate nucleus	10	14	2	3.63	0.105	128

Clusters of the parametric analysis. Effect of tDCS in the striatum using a flexible factorial design (time periods*groups). SPM maps were thresholded at $P_{uncorr} < 0.001$ at the voxel level, with a minimum of 10 contiguous voxels (80 mm^3). Only clusters with $P_{FWE} < 0.05$ at the cluster level were considered significant. We also reported the z-score at the peak level. The contrast reported here are [Active tDCS < Sham tDCS]. No significant clusters were reported with the contrast [Active tDCS > Sham tDCS]. The anatomical subparts of the striatum (i.e., caudate nucleus, putamen, and nucleus accumbens) were named based on the Hammersmith maximum probability brain atlas.

education, Motivation score, LOT-R score, BFI N score, STAI-difference, BP_R baseline) or the Wilcoxon rank sum test with continuity correction (age, STAI-A scores baseline and post, movement translation) and the Chi-squared test for handedness, sex variables, and blinding integrity. These analyses were done using in-house scripts in R (https://cran.r-project.org/).

Data and Code Availability

The data and custom-written analysis code that support the findings of this study are available on request from the corresponding author.

Results

Subjects' Characteristics

The subjects' characteristics are shown in Table 1 for both active and sham tDCS groups. No statistical differences were found between the 2 groups. As no distribution differences between groups (gender and age) were observed, we did not use them as covariables for the statistical calculations. No adverse effects were reported either due to the tDCS stimulation, the MRI, or the PET scans.

Kinetic Analysis

The extraction of the [^{11}C]raclopride binding potential ratio (BP_R) in the region of interest (striatum) (Fig. 2A) enabled us to determine a baseline time period during which BP_R reached a state close to equilibrium. The other time periods, that have been be used to create the mean ratio images for the parametric analysis, were of 15 min each. Thus, the effects of the stimulation have been examined over 4 time periods: Baseline period (30–40 min after tracer injection), Stimulation period (45–60 min, effects during stimulation), Post1 period (65–80 min, acute after-effects), Post2 period (80–95 min, subsequent after-effects). A baseline BP_R difference between the active and sham group in the striatum was reported ($P = 0.018$; Active 5.23 ± 0.51; Sham: 4.79 ± 0.46; mean ± SD). Therefore, subsequent analysis took this difference into account with comparisons of relative variations in each contrast.

Parametric Analysis

The analysis was performed using a mask of the whole striatum (a priori ROI). The voxel-based analysis showed significant clusters in the striatum when comparing the time periods determined between groups (Table 2). More specifically, when comparing active and sham tDCS groups, areas of significant changes in dopaminergic activity showed BP_R decreases in the striatum (Fig. 2B). After the complete analysis, the position of the significant clusters have been identified according to the anatomical subparts of the striatum delineation of Hammersmith maximum probability brain atlas, that is, the caudate nucleus, putamen, and nucleus accumbens. The [^{11}C]raclopride BP_R in clusters and their relative difference in the active tDCS group compared with the sham group are summarized in Table 3.

Effects of tDCS During the Stimulation (Stimulation Period)

No significant differences in BP_R were observed in the striatum when comparing stimulation and baseline periods, between groups $[(\text{Stimulation–Baseline})_{sham}$ vs. $(\text{Stimulation–Baseline})_{active}]$.

After-Effects of tDCS

During the 5–35-min period following the stimulation (Post1 + Post2 period). Significant differences in BP_R were reported in the active group compared with sham group when comparing the baseline period with the 5–35-min period following the stimulation $[((\text{Post1 + Post2})–\text{Baseline})_{sham}$ vs. $((\text{Post1 + Post2})–\text{Baseline})_{active}]$, specifically in the right caudate nucleus (–25.4%). Accordingly, a trend towards significance was also reported when comparing the stimulation period with the 5–35-min period following the stimulation $[((\text{Post1 + Post2})–\text{Stimulation})_{sham}$ vs. $((\text{Post1 + Post2})–\text{Stimulation})_{active}]$, specifically in the left putamen (–16.5%) and in the right caudate nucleus (–20.3%).

Table 3 [^{11}C]raclopride binding potential ratio in clusters

Cluster volume (mm^3)/ tDCS group		Raclopride BP_R, mean (±SD) Condition 1	Condition 2	Relative variation, %	Difference Active—Sham Group
Right caudate nucleus					
272		Baseline	Stimulation + Post1 + Post2		−22.46
	Active tDCS	5.78 (±0.88)	4.89 (±1.40)	−15.05 (±9.47)	
	Sham tDCS	4.93 (±1.01)	5.23 (±1.48)	7.41 (±14.79)	
352		Baseline	Post1 + Post2		−25.36
	Active tDCS	5.66 (±0.83)	4.55 (±1.28)	−19.05 (±9.86)	
	Sham tDCS	4.78 (±0.91)	5.02 (±1.39)	6.31 (±15.57)	
144		Stimulation	Post1 + Post2		−20.33
	Active tDCS	4.77 (±1.19)	4.18 (±1.74)	−11.73 (±21.18)	
	Sham tDCS	4.46 (±1.49)	4.84 (±2.05)	8.60 (±15.48)	
144		Stimulation	Post1		−33.82
	Active tDCS	3.99 (±1.30)	3.39 (±1.43)	−13.34 (±18.71)	
	Sham tDCS	3.35 (±1.09)	3.94 (±1.57)	20.48 (±26.03)	
360		Baseline	Post2		−31.97
	Active tDCS	5.64 (±0.92)	4.31 (±1.36)	−23.32 (±12.03)	
	Sham tDCS	4.82 (±0.89)	5.16 (±1.55)	8.65 (±19.90)	
128		Stimulation	Post2		−29.32
	Active tDCS	5.64 (±1.47)	4.52 (±2.04)	−19.02 (±25.83)	
	Sham tDCS	5.00 (±1.62)	5.47 (±2.45)	10.30 (±22.03)	
Left putamen					
160		Stimulation	Post1 + Post2		−16.49
	Active tDCS	7.91 (±2.13)	6.58 (±2.00)	−13.89 (±18.07)	
	Sham tDCS	6.81 (±2.03)	6.80 (±1.88)	2.60 (±19.96)	
192		Stimulation	Post1		−13.99
	Active tDCS	6.86 (±1.53)	5.78 (±1.52)	−13.99 (±21.78)	
	Sham tDCS	6.04 (±1.39)	6.00 (±1.55)	−0.00 (±18.03)	
128		Baseline	Post2		−25.9
	Active tDCS	4.89 (±0.94)	4.44 (±2.13)	−6.95 (±25.21)	
	Sham tDCS	4.43 (±0.86)	5.28 (±2.10)	18.95 (±23.71)	

[^{11}C]raclopride binding potential in clusters revealed by the parametric analysis—BP_R variations during and after the stimulation compared with baseline (relative variation, %). The anatomical subparts of the striatum (i.e., caudate nucleus, putamen, and nucleus accumbens) were named based on the Hammersmith maximum probability brain atlas.

Acute after-effects: during the 5–20-min period following the stimulation (Post1 period). No significant differences in BP_R were observed between groups in the striatum when comparing the baseline period with the 5–20-min period immediately following the stimulation [$(Post1–Baseline)_{sham}$ vs. $(Post1–Baseline)_{active}$].

However, when comparing the 5–20 min period immediately following the stimulation to the stimulation period [$(Post1–Stimulation)_{sham}$ vs. $(Post1–Stimulation)_{active}$], a trend towards a significant BP_R decrease was observed in the active group compared with sham group specifically in the left putamen (−14.0%) and in the right accumbens and caudate nuclei (−33.8%).

*Subsequent after-effects: during the 20–35-min period following the stimulation (Post2 period) Figure 2*B. Differences in BP_R were reported in the active group compared with sham group when comparing the baseline period with the 20–35-min period following the stimulation [$(Post2–Baseline)_{sham}$ vs. $(Post2–Baseline)_{active}$], specifically significant in the right caudate nucleus (−32.0%) and trending significance in the left putamen (−25.9%). Furthermore, a trend towards a significant differences was reported specifically in the right caudate nucleus (−29.3%) when comparing the stimulation period with the 20–35-min period following the stimulation [$(Post2–Stimulation)_{sham}$ vs. $(Post2–Stimulation)_{active}$].

Correlation Analysis

An analysis was performed in the cluster reported significant with the voxel-based parametric analysis, that is, in the right caudate nucleus, to investigate the impact of baseline dopamine BP_R levels on the relative BP_R difference (Delta (%)) between Post2 and Baseline time periods. This correlation analysis was not significant (active group: $r = 0.26$, $P = 0.37$; sham group: $r = 0.45$, $P = 0.061$) (Supplementary Fig. 1).

Discussion

Here, we present the first direct evidence of temporally and spatially distributed effects of bifrontal tDCS on dopamine transmission in the striatum after one session of 20 min at 2 mA, in healthy subjects. These results provide the first proof of a decrease in [^{11}C]raclopride BP_R suggesting an increase in extracellular dopamine induced by a dopamine release evoked by a tDCS session.

The impact on dopamine transmission seems progressive during the stimulation and reaches significance during the 5–35-min period following the end of stimulation. The absence of significant effects during the stimulation could be considered as contrasting with some previous online stimulation studies. In this line, glutamate/glutamine variations have been observed in the left striatum

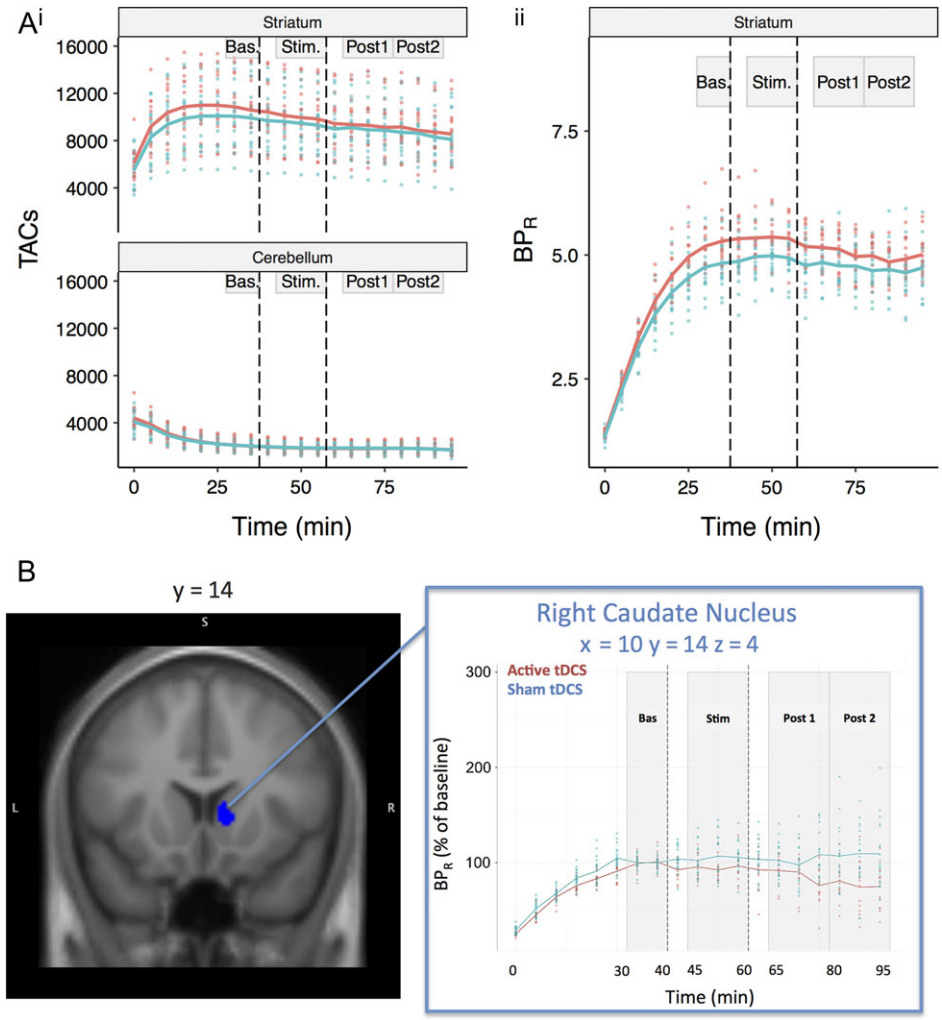

Figure 2. (*A*) Kinetic analysis. (i) Time–activity curve in the striatum and the cerebellum (ii) Binding potential ratio in the striatum; for both groups across the 20 PET frames (5 min per frame). (*B*) Parametric analysis—Subsequent after-effects of the stimulation in different clusters when comparing the baseline period to the Post2 period ($P_{uncorr} < 0.001$ at the voxel level, with a minimum of 10 contiguous voxels (80-mm^3)). For the significant cluster ($P_{FWE} < 0.05$ at the cluster level), the BP_R kinetic curves for both groups across the 20 PET frames (5 min per frame) are extracted and are expressed as BP_R ratio (% of baseline). The anatomical subparts of the striatum (i.e., caudate nucleus, putamen, and nucleus accumbens) were named based on the Hammersmith maximum probability brain atlas. Abbreviations: Bas., Baseline period; Stim, Stimulation period; Red curve, Active tDCS; Blue curve, Sham tDCS, BP_R, Binding Potential Ratio; TACs, Time–Activity Curves.

during a single bifrontal tDCS session using online MRS (Hone-Blanchet et al. 2016). The discrepancy with our results could be explained by several factors. First, regarding technical features, MRS measures a mixture of compounds involved in neurotransmission and metabolism in every cellular compartment of the voxel. Here, with [^{11}C]raclopride PET, we addressed dopamine neurotransmission in terms of extracellular dopamine. Second, regarding physiological features, it cannot be ruled out that the time-scale of glutamate and dopamine variations is different. With this hypothesis, changes in the macro- and microenvironment induced during tDCS could trigger dopamine release only when the stimulation ends. Another explanation could be a matter of significant threshold. Indeed, the BP_R curve over time (Fig. 2*B*) shows a continuous decrease starting at the beginning of the stimulation, only for the active tDCS group. However, this decrease reaches significance only after the end of the stimulation compared with the sham group.

The increase in dopamine is in line with studies exploring TMS impact on dopamine transmission in animals, healthy subjects and in pathological conditions, as well as tDCS in animals (Ko and Strafella 2012). These studies conducted offline showed modulations of dopamine transmission in the striatum after stimulation protocols applied over the prefrontal cortex. For example, an increase in extracellular dopamine specifically in the left dorsal caudate nucleus was shown after a repetitive TMS stimulation with the coil over the left DLPFC (Strafella et al. 2001). In the same line, an animal tDCS study reported an increase in dopamine concentration in rat basal ganglia after cathodal tDCS compared with sham and anodal conditions. The effect was significant from 120 min after the stimulation (Tanaka et al. 2013).

The significant clusters identified in our study are localized specifically in the ventral regions of the striatum. This spatially distributed after-effect of bifrontal tDCS is supported by the notion that complex organized behavior is made possible by the connectivity between several striato-thalamo-cortical circuits, including distinct striatal and cortical regions (Haber and Knutson 2010). Several studies have highlighted the model of a tripartite division of the striatum (Postuma 2005; Di Martino et al. 2008; Draganski et al. 2008; Pauli et al. 2016), using noninvasive neuroimaging

methods. This striatal parcellation corresponds to 3 functionally distinct regions: a motor region which includes the dorsal part of the putamen and caudate nucleus, a cognitive region including the ventral rostral putamen, dorsal caudate, superior ventral striatum corresponding to the ventral caudate, and an affective region composed of the inferior ventral striatum or nucleus accumbens. In addition, connectivity studies have traced the structural and functional coupling between individual striatal and cortical regions and have shown that the DLPFC projects extensively to the ventral striatum, an overlap between regions involved in affective and cognitive processes, corresponding to the reward–motivation network. According to these studies, our clusters are located in the cognitive and affective regions of the striatum, regions anatomically linked to the DLPFC targeted by the tDCS montage.

Our findings of an increase in extracellular dopamine spatially located in the ventral striatum, obtained after a single session of bifrontal tDCS, are in line with the possible procognitive effects seen after frontal tDCS in healthy subjects and in pathological conditions (Kuo and Nitsche 2015; Lefaucheur et al. 2017). Indeed, multiple studies focused on the reciprocal influence of cognitive functions and variations in dopamine. Imaging studies have detected increases in ventral striatal extracellular dopamine concentrations during task components such as motor learning and execution, reward-related processes, stress, and cognitive performance (Egerton et al. 2009). Moreover, predictions about anticipated future rewarding have been shown to be encoded by dopamine concentration of the ventral striatum, and that the amount of dopamine itself encodes the distance from the reward (Howe et al. 2013). In the same line, manipulations that enhance dopamine transmission, such as addictive drugs and dopamine agonists, often act as neuroenhancers (Wise 2004; Nutt et al. 2015). However, as with pharmacological neuroenhancers, tDCS could also be linked to a direct dopamine release within the prefrontal cortex. We acknowledge that our study did not allow for an evaluation of the tDCS effects on dopamine release in the prefrontal cortex. Using a high affinity radioligand ([^{11}C]FLB-457), Cho and Strafella (2009) have shown that TMS over the left DLPFC induces a reduction of BP in the ipsilateral pre- and subgenual anterior cingulate cortex, and medial orbitofrontal cortex. Further studies are needed to evaluate the direct effect of tDCS on the prefrontal cortex.

The significant after-effects of bifrontal tDCS beg the question of possible mechanisms leading to the dopamine release in the striatum. The literature supports 2 possible mechanisms, involving glutamatergic cortical projections: a direct pathway, via corticostriatal projections and an indirect pathway, involving cortical projections on mesostriatal dopamine neurons in the midbrain. Both mechanisms could be involved in tDCS effects, according to animal studies showing that stimulation of the PFC could promote activation in both striatal and ventral tegmental regions (Taber and Fibiger 1995; Peanlikhit et al. 2017). With the notion that tDCS modulates glutamatergic and GABAergic activity under the electrodes (Stagg et al. 2009), bifrontal tDCS may impact the glutamatergic projections from the DLPFC, and consequently modify subcortical activity, as shown by a recent MR-spectroscopy study reporting that bifrontal tDCS had fast excitatory effects in the left striatum (Hone-Blanchet et al. 2016). To further investigate the exact mechanism, future studies could explore the impact of bifrontal tDCS on the relation between blood flow and dopamine transmission variations.

Based on our results and according to the increasing use of tDCS in various populations, the level of dopamine signaling should be considered for each tDCS application. Indeed, it is important to note that the subject's brain-state at the time of stimulation plays an important role in the response (Silvanto and Pascual-Leone 2008). Accordingly, effects of bifrontal tDCS could be sensitive to the level of dopamine activity at baseline. An inverted U-shape hypothesis has been put forth describing a nonlinear relationship between cognitive performance and dopamine concentration. Both too high as well as too low concentrations of dopamine are associated with suboptimal cognitive processing (Cools and D'Esposito 2011). Pharmacological studies suggest a similar relationship between dopaminergic activity and neuroplastic changes induced by tDCS applied over the human motor cortex (Kuo et al. 2008; Monte-Silva et al. 2010; Fresnoza et al. 2014). A recent review has reported that the modulation of dopamine D1 and D2 signaling by agonist and antagonist administration has a significant dose and receptor-dependent impact on tDCS after-effects (McLaren et al. 2018). Combined with our results, a reciprocal interaction between dopaminergic systems and tDCS can be suggested.

Therefore, exploring the effects of bifrontal tDCS under conditions where basal dopamine activity is altered could be of major relevance. First, in psychiatric conditions such as depression, stimulation studies robustly report groups of responders and nonresponders to repeated bifrontal tDCS while physiological levels of dopamine activity have been shown heterogeneous across subjects (Seamans and Yang 2004). According to our results, it can be hypothesized that the basal dopamine activity level or the change in extracellular dopamine evoked by a first bifrontal tDCS session could be a predictive marker of the therapeutic response obtained after applying multiple tDCS sessions on several days, protocol used in studies developing tDCS as a treatment for psychiatric disorders. Second, tDCS devices are being increasingly used in a recreational manner with little or no warning to interaction with medication or psychostimulant, in particular those interacting with the dopamine transmission. However in our study, we did not observe any impact of the baseline dopamine levels on the release induced by tDCS. Nevertheless, our study included only healthy subjects at rest and free of treatment interfering with dopaminergic transmission. From this, it could be suggested that, in these specific population and conditions, the intersubjects difference in dopamine activity may not impact tDCS effects. Overall, our work shows the ongoing importance of controlled studies when using tDCS and should boost the research in this field to prevent the unsafe use of tDCS in uninformed people.

One limitation of this study is that PET results were not associated with behavioral findings (e.g., improvement of working memory performances), hence no procognitive effects were in fact inspected in the present study. The second limitation is that dopamine has also been shown to be involved in placebo responsiveness (Benedetti 2014). The placebo-controlled study design developed here overcame in part this problem. Moreover, the psychological assessment conducted did not reveal differences between active and sham groups regarding personality traits, motivation, and anxiety.

To conclude, the present study provides first direct evidence that bifrontal tDCS induces neurotransmitter release in polysynaptic connected subcortical areas. Our findings offer new insights for innovative use of tDCS as a therapeutic solution in neuropsychiatric conditions involving dopamine transmission impairments in the reward–motivation network. In the context of the ongoing debate surrounding tDCS in the literature and beyond the simple "excitatory–inhibitory" model, levels of dopamine activity and reactivity should be a new element of the mosaic, adding to other parameters such as individual

head anatomy variability, electrode position, and brain-state dependency for a general hypothesis of brain modulation by bifrontal tDCS (Krause and Cohen Kadosh 2014; Opitz et al. 2015; Wörsching et al. 2016).

Supplementary Material

Supplementary material is available at *Cerebral Cortex* online.

Funding

This work was supported by a grant from the "Conseil Scientifique de la Recherche" from the Vinatier hospital, Bron, France. The funding source had no further role in the study design; in the collection, analysis, and interpretation of data; in the writing of the report; and in the decision to submit the paper for publication.

Notes

The authors thank C. Tourvieille, F. Bonnefoi, F. Liger, T. Iecker, F. Cadarossanesaib for their help in preparation of the radiotracer, Dr P. Vignaud and Dr F. Galvao for the subjects' inclusion, and V. Berthier, C. Vighi, A. Maurin and E. Greusard for their help for the MRI and PET acquisitions. *Conflict of Interest*: None declared.

References

Adler CM, Elman I, Weisenfeld N, Kestler L, Pickar D, Breier A. 2000. Effects of acute metabolic stress on striatal dopamine release in healthy volunteers. Neuropsychopharmacology. 22:545–550.

Bai S, Dokos S, Ho K-A, Loo C. 2014. A computational modelling study of transcranial direct current stimulation montages used in depression. NeuroImage. 87:332–344.

Benedetti F. 2014. Placebo effects: from the neurobiological paradigm to translational implications. Neuron. 84:623–637.

Bindman LJ, Lippold OCJ, Redfearn JWT. 1964. The action of brief polarizing currents on the cerebral cortex of the rat (1) during current flow and (2) in the production of long-lasting after-effects. J Physiol. 172:369.

Bromberg-Martin ES, Matsumoto M, Hikosaka O. 2010. Dopamine in motivational control: rewarding, aversive, and alerting. Neuron. 68:815–834.

Brunelin J, Fecteau S, Suaud-Chagny M-F. 2013. Abnormal striatal dopamine transmission in schizophrenia. Curr Med Chem. 20:397–404.

Brunelin J, Szekely D, Costes N, Mondino M, Bougerol T, Saoud M, Suaud-Chagny M-F, Poulet E, Polosan M. 2011. Theta burst stimulation in the negative symptoms of schizophrenia and striatal dopamine release. Schizophr Res. 131: 264–265.

Brunoni AR, Amadera J, Berbel B, Volz MS, Rizzerio BG, Fregni F. 2011. A systematic review on reporting and assessment of adverse effects associated with transcranial direct current stimulation. Int J Neuropsychopharmacol. 14:1133–1145.

Brunoni AR, Moffa AH, Fregni F, Palm U, Padberg F, Blumberger DM, Daskalakis ZJ, Bennabi D, Haffen E, Alonzo A, et al. 2016. Transcranial direct current stimulation for acute major depressive episodes: meta-analysis of individual patient data. Br J Psychiatry. 208:522–531.

Brunoni AR, Moffa AH, Sampaio-Junior B, Borrione L, Moreno ML, Fernandes RA, Veronezi BP, Nogueira BS, Aparicio LVM, Razza LB, et al. 2017. Trial of electrical direct-current therapy versus escitalopram for depression. N Engl J Med. 376:2523–2533.

Cho SS, Strafella AP. 2009. rTMS of the left dorsolateral prefrontal cortex modulates dopamine release in the ipsilateral anterior cingulate cortex and orbitofrontal cortex. PLoS One. 4:e6725.

Cools R. 2011. Dopaminergic control of the striatum for high-level cognition. Curr Opin Neurobiol. 21:402–407.

Cools R, D'Esposito M. 2011. Inverted-U–shaped dopamine actions on human working memory and cognitive control. Biol Psychiatry. 69:e113–e125.

Di Martino A, Scheres A, Margulies DS, Kelly AMC, Uddin LQ, Shehzad Z, Biswal B, Walters JR, Castellanos FX, Milham MP. 2008. Functional connectivity of human striatum: a resting state fMRI study. Cereb Cortex. 18:2735–2747.

Draganski B, Kherif F, Kloppel S, Cook PA, Alexander DC, Parker GJM, Deichmann R, Ashburner J, Frackowiak RSJ. 2008. Evidence for segregated and integrative connectivity patterns in the human basal ganglia. J Neurosci. 28:7143–7152.

Egerton A, Mehta MA, Montgomery AJ, Lappin JM, Howes OD, Reeves SJ, Cunningham VJ, Grasby PM. 2009. The dopaminergic basis of human behaviors: a review of molecular imaging studies. Neurosci Biobehav Rev. 33:1109–1132.

Fresnoza S, Stiksrud E, Klinker F, Liebetanz D, Paulus W, Kuo M-F, Nitsche MA. 2014. Dosage-dependent effect of dopamine D2 receptor activation on motor cortex plasticity in humans. J Neurosci. 34:10701–10709.

Friston KJ, Frith CD, Liddle PF, Frackowiak RSJ. 1991. Comparing functional (PET) images: the assessment of significant change. J Cereb Blood Flow Metab. 11:690–699.

Gousias IS, Rueckert D, Heckemann RA, Dyet LE, Boardman JP, Edwards AD, Hammers A. 2008. Automatic segmentation of brain MRIs of 2-year-olds into 83 regions of interest. NeuroImage. 40:672–684.

Guay F, Mageau GA, Vallerand RJ. 2003. On the hierarchical structure of self-determined motivation: a test of top-down, bottom-up, reciprocal, and horizontal effects. Pers Soc Psychol Bull. 29:992–1004.

Haber SN, Knutson B. 2010. The reward circuit: linking primate anatomy and human imaging. Neuropsychopharmacology. 35:4–26.

Hall H, Kohler C, Gawell L, Farde L, Sedvall G. 1988. Raclopride, a new selective ligand for the dopamine-D2 receptors. Prog Neuropsychopharmacol Biol Psychiatry. 12:559–568.

Hammers A, Allom R, Koepp MJ, Free SL, Myers R, Lemieux L, Mitchell TN, Brooks DJ, Duncan JS. 2003. Three-dimensional maximum probability atlas of the human brain, with particular reference to the temporal lobe. Hum Brain Mapp. 19: 224–247.

Hanganu A, Provost J-S, Monchi O. 2015. Neuroimaging studies of striatum in cognition part II: Parkinson's disease. Front Syst Neurosci. 9:138.

Hone-Blanchet A, Edden RA, Fecteau S. 2016. Online effects of transcranial direct current stimulation in real time on human prefrontal and striatal metabolites. Biol Psychiatry. 80:432–438.

Horvath JC, Forte JD, Carter O. 2015. Evidence that transcranial direct current stimulation (tDCS) generates little-to-no reliable neurophysiologic effect beyond MEP amplitude modulation in healthy human subjects: a systematic review. Neuropsychologia. 66:213–236.

Howe MW, Tierney PL, Sandberg SG, Phillips PEM, Graybiel AM. 2013. Prolonged dopamine signalling in striatum signals proximity and value of distant rewards. Nature. 500:575–579.

Jakoby BW, Bercier Y, Conti M, Casey ME, Bendriem B, Townsend DW. 2011. Physical and clinical performance of the mCT time-of-flight PET/CT scanner. Phys Med Biol. 56:2375–2389.

Jansen JM, Daams JG, Koeter MWJ, Veltman DJ, van den Brink W, Goudriaan AE. 2013. Effects of non-invasive neurostimulation on craving: a meta-analysis. Neurosci Biobehav Rev. 37:2472–2480.

Keeser D, Meindl T, Bor J, Palm U, Pogarell O, Mulert C, Brunelin J, Moller H-J, Reiser M, Padberg F. 2011. Prefrontal transcranial direct current stimulation changes connectivity of resting-state networks during fMRI. J Neurosci. 31:15284–15293.

Ko JH, Strafella AP. 2012. Dopaminergic neurotransmission in the human brain: new lessons from perturbation and imaging. The Neuroscientist. 18:149–168.

Krause B, Cohen Kadosh R. 2014. Not all brains are created equal: the relevance of individual differences in responsiveness to transcranial electrical stimulation. Front Syst Neurosci. 8:25.

Kuo M-F, Nitsche MA. 2015. Exploring prefrontal cortex functions in healthy humans by transcranial electrical stimulation. Neurosci Bull. 31:198–206.

Kuo M-F, Paulus W, Nitsche MA. 2008. Boosting focally-induced brain plasticity by dopamine. Cereb Cortex. 18:648–651.

Kuo M-F, Paulus W, Nitsche MA. 2014. Therapeutic effects of non-invasive brain stimulation with direct currents (tDCS) in neuropsychiatric diseases. NeuroImage. 85:948–960.

Lefaucheur J-P, Antal A, Ayache SS, Benninger DH, Brunelin J, Cogiamanian F, Cotelli M, De Ridder D, Ferrucci R, Langguth B, et al. 2017. Evidence-based guidelines on the therapeutic use of transcranial direct current stimulation (tDCS). Clin Neurophysiol. 128:56–92.

Leite J, Gonçalves OF, Carvalho S. 2014. Facilitative effects of bihemispheric tDCS in cognitive deficits of Parkinson disease patients. Med Hypotheses. 82:138–140.

Levasseur-Moreau J, Brunelin J, Fecteau S. 2013. Non-invasive brain stimulation can induce paradoxical facilitation. Are these neuroenhancements transferable and meaningful to security services? Front Hum Neurosci. 7:449.

Lindquist KA, Wager TD, Kober H, Bliss-Moreau E, Barrett LF. 2012. The brain basis of emotion: a meta-analytic review. Behav Brain Sci. 35:121–143.

Loo CK, Husain MM, McDonald WM, Aaronson S, O'Reardon JP, Alonzo A, Weickert CS, Martin DM, McClintock SM, Mohan A, et al. 2018. International randomized-controlled trial of transcranial direct current stimulation in depression. Brain Stimulat. 11:125–133.

Maia TV, Frank MJ. 2017. An integrative perspective on the role of dopamine in schizophrenia. Biol Psychiatry. 81:52–66.

McLaren ME, Nissim NR, Woods AJ. 2018. The effects of medication use in transcranial direct current stimulation: a brief review. Brain Stimulat. 11:52–58.

Monchi O, Petrides M, Strafella AP, Worsley KJ, Doyon J. 2006. Functional role of the basal ganglia in the planning and execution of actions. Ann Neurol. 59:257–264.

Mondino M, Thiffault F, Fecteau S. 2015. Does non-invasive brain stimulation applied over the dorsolateral prefrontal cortex non-specifically influence mood and emotional processing in healthy individuals? Front Cell Neurosci. 9:399.

Monte-Silva K, Liebetanz D, Grundey J, Paulus W, Nitsche MA. 2010. Dosage-dependent non-linear effect of l -dopa on human motor cortex plasticity: non-linear effect of l-dopa on plasticity. J Physiol. 588:3415–3424.

Nitsche MA, Seeber A, Frommann K, Klein CC, Rochford C, Nitsche MS, Fricke K, Liebetanz D, Lang N, Antal A, et al. 2005. Modulating parameters of excitability during and after transcranial direct current stimulation of the human motor cortex: cortical excitability and tDCS. J Physiol. 568:291–303.

Nutt DJ, Lingford-Hughes A, Erritzoe D, Stokes PRA. 2015. The dopamine theory of addiction: 40 years of highs and lows. Nat Rev Neurosci. 16:305–312.

Opitz A, Paulus W, Will S, Antunes A, Thielscher A. 2015. Determinants of the electric field during transcranial direct current stimulation. NeuroImage. 109:140–150.

Palm U, Keeser D, Hasan A, Kupka MJ, Blautzik J, Sarubin N, Kaymakanova F, Unger I, Falkai P, Meindl T, et al. 2016. Prefrontal transcranial direct current stimulation for treatment of schizophrenia with predominant negative symptoms: a double-blind, sham-controlled proof-of-concept study. Schizophr Bull. 42:1253–1261.

Pauli WM, O'Reilly RC, Yarkoni T, Wager TD. 2016. Regional specialization within the human striatum for diverse psychological functions. Proc Natl Acad Sci. 113:1907–1912.

Peanlikhit T, Van Waes V, Pedron S, Risold P-Y, Haffen E, Etiévant A, Monnin J. 2017. The antidepressant-like effect of tDCS in mice: a behavioral and neurobiological characterization. Brain Stimulat. 10(4):748–756.

Pena-Gomez C, Sala-Lonch R, Junque C, Clemente IC, Vidal D, Bargallo N, Falcon C, Valls-Sole J, Pascual-Leone A, Bartres-Faz D. 2012. Modulation of large-scale brain networks by transcranial direct current stimulation evidenced by resting-state functional MRI. Brain Stimulat. 5:252–263.

Pinborg LH, Videbaek C, Ziebell M, Mackeprang T, Friberg L, Rasmussen H, Knudsen GM, Glenthoj BY. 2007. [123I]epidepride binding to cerebellar dopamine D2/D3 receptors is displaceable: implications for the use of cerebellum as a reference region. NeuroImage. 34:1450–1453.

Plaisant O, Courtois R, Réveillère C, Mendelsohn GA, John OP. 2010. Validation par analyse factorielle du Big Five Inventory français (BFI-Fr). Analyse convergente avec le NEO-PI-R. Ann Méd-Psychol Rev Psychiatr. 168:97–106.

Postuma RB. 2005. Basal ganglia functional connectivity based on a meta-analysis of 126 positron emission tomography and functional magnetic resonance imaging publications. Cereb Cortex. 16:1508–1521.

Price JL, Drevets WC. 2012. Neural circuits underlying the pathophysiology of mood disorders. Trends Cogn Sci. 16: 61–71.

Sampaio-Junior B, Tortella G, Borrione L, Moffa AH, Machado-Vieira R, Cretaz E, Fernandes da Silva A, Fraguas R, Aparício LV, Klein I, et al. 2018. Efficacy and safety of transcranial direct current stimulation as an add-on treatment for bipolar depression: a randomized clinical trial. JAMA Psychiatry. 75:158.

Seamans JK, Yang CR. 2004. The principal features and mechanisms of dopamine modulation in the prefrontal cortex. Prog Neurobiol. 74:1–58.

Silvanto J, Pascual-Leone A. 2008. State-dependency of transcranial magnetic stimulation. Brain Topogr.. 21:1–10.

Spielberger CD, Gorsuch RL, Lushene RE. 1970. Manual for the state-trait anxiety inventory.

Stagg CJ, Best JG, Stephenson MC, O'Shea J, Wylezinska M, Kincses ZT, Morris PG, Matthews PM, Johansen-Berg H. 2009. Polarity-sensitive modulation of cortical neurotransmitters by transcranial stimulation. J Neurosci. 29:5202–5206.

Strafella AP, Paus T, Barrett J, Dagher A. 2001. Repetitive transcranial magnetic stimulation of the human prefrontal cortex induces dopamine release in the caudate nucleus. J Neurosci. 21:1–4.

Taber MT, Fibiger HC. 1995. Electrical stimulation of the prefrontal cortex increases dopamine release in the nucleus accumbens of the rat: modulation by metabotropic glutamate receptors. J Neurosci. 15:3896–3904.

Tanaka T, Takano Y, Tanaka S, Hironaka N, Kobayashi K, Hanakawa T, Watanabe K, Honda M. 2013. Transcranial direct-current stimulation increases extracellular dopamine levels in the rat striatum. Front Syst Neurosci. 7:6.

Trottier C, Mageau G, Trudel P, Halliwell WR. 2008. Validation de la version canadienne-française du Life Orientation Test-Revised. Can J Behav Sci Rev Can Sci Comport. 40:238–243.

Wise RA. 2004. Dopamine, learning and motivation. Nat Rev Neurosci. 5:483–494.

Wörsching J, Padberg F, Ertl-Wagner B, Kumpf U, Kirsch B, Keeser D. 2016. Imaging transcranial direct current stimulation (tDCS) of the prefrontal cortex—correlation or causality in stimulation-mediated effects? Neurosci Biobehav Rev. 69:333–356.

Wörsching J, Padberg F, Helbich K, Hasan A, Koch L, Goerigk S, Stoecklein S, Ertl-Wagner B, Keeser D. 2017. Test-retest reliability of prefrontal transcranial Direct Current Stimulation (tDCS) effects on functional MRI connectivity in healthy subjects. NeuroImage. 155:187–201.